Simultaneous low extinction and high local field enhancement in Ag nanocubes

2011 Chinese Phys. B 20 037303

(http://iopscience.iop.org/1674-1056/20/3/037303)

Rapid Communication

Simultaneous low extinction and high local field enhancement in Ag nanocubes*

Zhou Fei(周 飞)[a], Liu Ye(刘 晔)[a,b], and Li Zhi-Yuan(李志远)[a,†]

[a] *Laboratory of Optical Physics, Institute of Physics, Chinese Academy of Sciences, Beijing* 100190, *China*
[b] *Anhui Provincial Key Lab of Photonics Devices and Materials, Anhui Institute of Optics and Fine Mechanics, Chinese Academy of Sciences, Hefei* 230031, *China*

(Received 13 October 2010; revised manuscript received 12 November 2010)

We theoretically investigate surface plasmon resonance properties in Au and Ag cubic nanoparticles and find a novel plasmonic mode that exhibits simultaneous low extinction and high local field enhancement properties. We analyse this mode from different aspects by looking at the distribution patterns of local field intensity, energy flux, absorption and charge density. We find that in the mode the polarized charge is highly densified in a very limited volume around the corner of the nanocube and results in very strong local field enhancement. Perturbations of the incident energy flux and light absorption are also strongly localized in this small volume of the corner region, leading to both low absorption and low scattering cross section. As a result, the extinction is low for the mode. Metal nanoparticles involving such peculiar modes may be useful for constructing nonlinear compound materials with low linear absorption and high nonlinearity.

Keywords: surface plasmon resonance, low extinction, local field enhancement
PACS: 73.20.Mf, 78.67.Bf **DOI:** 10.1088/1674-1056/20/3/037303

1. Introduction

In recent years, significant attention has been paid to the study of metal nanoparticles for their application in nonlinear coefficient enhancement,[1−3] destruction of cancer cells,[1−4] detection,[5,6] surface-enhanced Raman scattering (SERS)[7−10] and many others.[11−14] The role of localized surface plasmon resonance (LSPR) in these applications has been clearly established for many years.[7,15] It is generally accepted that the local field enhancement will be maximized when the incident light wavelength is in resonance with the LSPR band of the nanoparticle.[16,17] However, when LSPR takes place, light extinction is also strong, and this reduces the lifetime of the LSPR mode and the corresponding figure of merit (FOM). Thus it is worthwhile to find a resonant mode with both a large field enhancement and low extinction. Many methods have been proposed to solve this problem from either a theoretical or an experimental angle. Siu and Yu[18] showed that when nanoparticles are anisotropically arranged in their geometry, optical nonlinearity is enhanced. Further, Yuen *et al.*[19] showed that anisotropic composite media can separate the absorption peak from the nonlinear enhancement peak, thereby greatly enhancing the FOM. Wang *et al.*[20] introduced a Fe nanoparticle to quench the LSPR peak, which could effectively enhance the FOM. Recently, McMahon *et al.*[10] found a high local field enhancement at extinction minimum using gold nanoparticles dimer simulated with two-dimensional model. In the present article we present a new scheme to simultaneously attain a low extinction cross section and a large local field enhancement.

Noble metal nanocubes have received much attention both theoretically and experimentally due to their excellent properties.[21−26] Recently we found that simple Au and Ag cubic nanoparticles can exhibit a special resonance mode where the extinction cross section is much lower than those of other LSPR modes, while the local field enhancement factor is at a considerably high level. This feature may be very useful for practical applications such as SERS and nonlinear enhancement. We analyse the physical mechanism behind the peculiar feature of this large field enhancement and low extinction (LFE-LE) resonance mode in detail.

*Project supported by the National Natural Science Foundation of China (Grant Nos. 60736041 and 10874238), and the National Key Basic Research Special Foundation of China (Grant No. 2007CB613205).
†Corresponding author. E-mail: lizy@aphy.iphy.ac.cn

2. Existence of LFE-LE modes

We first consider an Ag nanocube with an edge length of 150 nm embedded in water, as schematically depicted in Fig. 1.

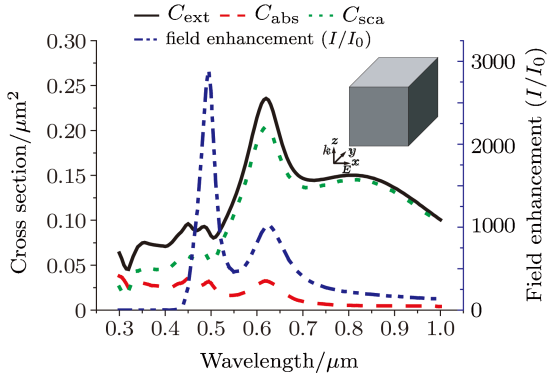

Fig. 1. (Colour online) Calculated optical cross section spectra for the Ag nanocube embedded in a water background with an edge length of 150 nm. The black solid, red dash and green dot lines correspond to extinction, absorption and scattering cross sections, respectively. The field enhancement factor (I/I_0) is also plotted (blue line). The inter-dipole spacing in simulation is 1.5 nm. The schematic configuration of the nanocube and the coordinate system for the simulation are also indicated in the figure.

We adopt the discrete-dipole approximation (DDA) method[27,28] to study this nanosystem by extensive numerical simulations. The grid size in the DDA method is chosen to be 1.5 nm and the total dipole number used to represent the cubic particle is 1,000,000. Sufficient numerical convergence has been achieved and discussed in the Appendix. The incident light is a plane wave irradiated from the bottom of the nanocube, i.e., the [001] direction, and the electric field is polarized along the edge of the nanocube, i.e., the [100] direction. The simulation results of the extinction cross section and the maximum field enhancement factor of the cubic nanoparticle, each as a function of illumination wavelength, are shown in Fig. 1. We find that the field enhancement peak of 495 nm only corresponds to the low region of the extinction curve. This means that at this wavelength, the electric field can be enhanced efficiently, while the loss is relatively low. On the long wavelength side of this field enhancement peak, there are two dominant SPR peaks located at 810 nm and 620 nm, which correspond to dipole and quadrupole SPR modes, according to our recent mode classification theory presented in Ref. [27]. The extinction cross section at the field enhancement peak is half of the dipole mode and one-third of the quadrupole mode, but the maximum local field enhancement factor, which is defined as I/I_0, where I and I_0 are the local field intensity and incident field intensity, respectively, is 14 times and 2.8 times the values of the dipole mode and the quadrupole mode, respectively.

To justify the result, we further simulate a series of Au and Ag nanocube structures that have different sizes and are embedded in both air and water background media. The results are summarized in Fig. 2. The spectra of optical cross sections and maximum field enhancement factor are all plotted in the same figure for comparison. The three columns, from left to right, correspond to three different setups, which are Ag nanocube embedded in air, Ag nanocube in water and Au nanocube in water. The three rows, from top to bottom, correspond to the edge lengths of 100 nm, 150 nm and 200 nm, respectively. All the results are simulated using 10^8 dipoles. From Fig. 2, we find that some nanocubes also have an obvious field enhancement peak, which does not correspond to any extinction cross section peak. When the nanocube is small, this peak is hardly recognizable (see the first row) and may overlap other peaks. But for the bigger nanocube (see the second row and the third row), this peak is obvious and its field enhancement factor may be even larger than those of the resonant extinction peaks. For example, we look at the 200 nm Ag nanocube placed in water (see Fig. 2(h)), the field enhancement factor at the peak of 505 nm peak is much larger than that at the peak of 750 nm. With a small extinction cross section, the peak at 505 nm is an LFE-LE peak.

Comparing the two figures in each row of the first two columns, we can find that with the same size of Ag nanocube, the results in the second column (nanocube in water) show a more obvious LFE-LE peak than in the first column (nanocube in air). This is because the light wavelength gets shorter in water, i.e., the effective size of the nanocube is bigger in water than in air, and this phenomenon will be more obvious at a larger size. When we change the metal material from Ag to Au (comparing the second column and the third column in Fig. 2), the LFE-LE peak still exists. However, because the dispersion is dependent on material characteristics, different wavelengths and field enhancement factors of the LFE-LE mode are observed. There is another interesting phenomenon: the position of LFE-LE peak is not sensitive to the size of nanocube. When the edge length of the nanocube increases from 100 nm to 200 nm, the quadrupole mode peak red-shifts by more than 100 nm, but the LFE-LE peak only slightly red-shifts (see each column in Fig. 2).

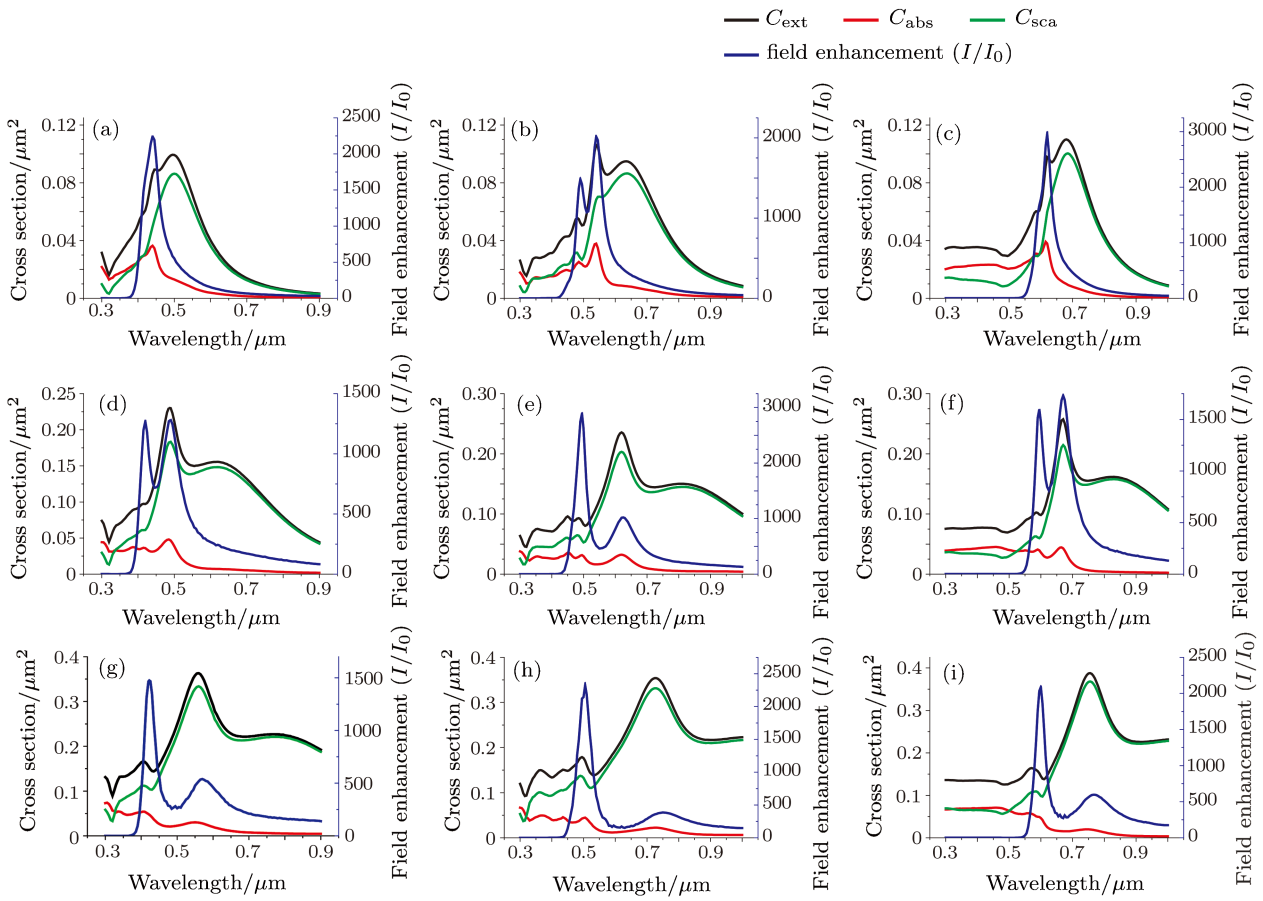

Fig. 2. (Colour online) Optical cross sections (the black solid lines represent extinction cross sections, the red and green lines denote absorption and scattering cross section, respectively) and the maximum field enhancement factor (I/I_0) (blue lines). The first row represents a nanocube with an edge length of 100 nm and the following two rows are for nanocubes with edge lengths of 150 nm and 200 nm, respectively. The column on the left is for Ag nanocubes placed in air, while the cases for Ag particles in water and Au particles in water are shown in the central column and the right column, respectively.

3. Physical mechanism of the LFE-LE mode

So far we have seen that both Ag and Au nanocubes can achieve the properties of simultaneous large field enhancement factor and low extinction cross section at a certain wavelength. Such a property is very different from those of the quadrupole mode peak and dipole mode peak. In the following, we try to analyse the physical mechanism of this strange peak in detail. For simplicity, we adopt the system with a 150 nm long Ag nanocube embedded in water (whose optical spectrum has been illustrated in Fig. 2(e) or Fig. 1). In this system, there are three peaks in the spectrum, which are located at 495 nm, 620 nm and 815 nm, respectively.

It has been well established from numerous experiences that electromagnetic field distribution can offer a good clue to many optical phenomena. So we first take a close look at the electric field patterns corresponding to the three peaks. In most cases, this concerns the electric field enhancement around the nanocube. So we select an outer plane parallel to the right surface of the nanocube with a gap of 2 nm (see Fig. 3(d)), in which the electric field is calculated. The electric field distributions at the wavelengths of 495, 620 and 815 nm are shown in Figs. 3(a)–3(c), respectively. At the wavelength of 495 nm, the maximum field enhancement factor is 2891 and the field enhancement effect is highly localized in the region that is very close to the corner. For the wavelength of 620 nm, the maximum field enhancement factor is reduced down to 1020, while the field enhancement effect takes place in a larger volume near the corner. For the wavelength of 815 nm, the maximum field enhancement factor is as low as 208, but the field enhancement effect almost covers half the surface of the nanocube. To go

further, we calculate the electric charge density distribution in each case by the DDA method and the results are shown in Fig. 4. It is very obvious that at the wavelength of 620 nm, it is a quadrupole mode, whose positive and negative charges are distributed in the corners alternately (see Fig. 4(c)). At the wavelength of 815 nm, it is a dipole resonant mode because the charges are mainly concentrated in the upper corners but with opposite signs on the two sides (see Fig. 4(d)).

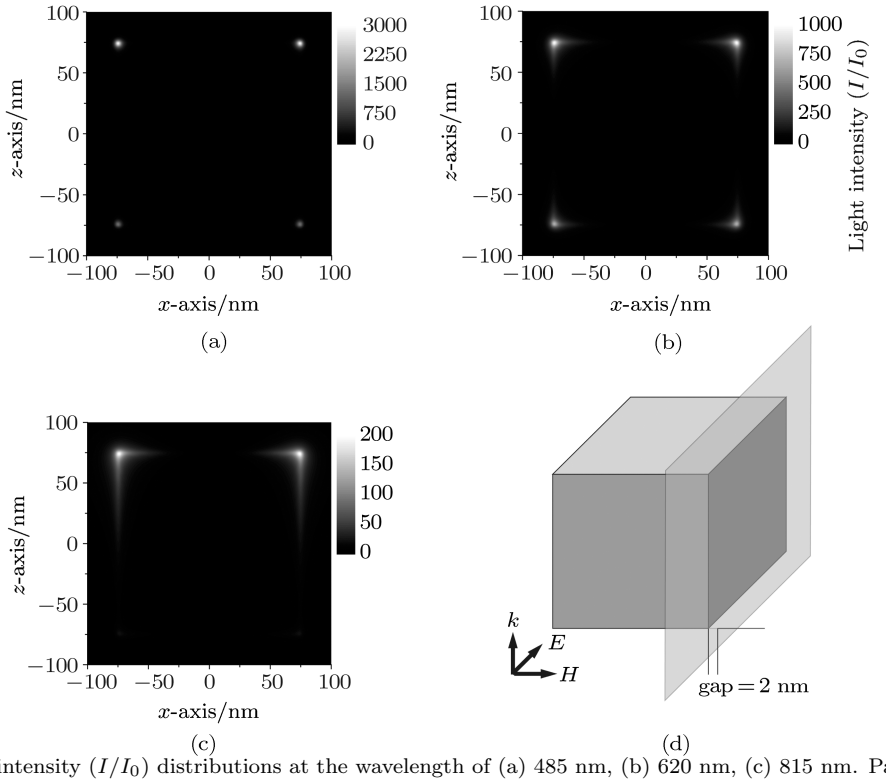

Fig. 3. Light intensity (I/I_0) distributions at the wavelength of (a) 485 nm, (b) 620 nm, (c) 815 nm. Panel (d) shows the surface within which the electric field pattern is calculated and plotted. The gap between the surface and the nanocube is 2 nm.

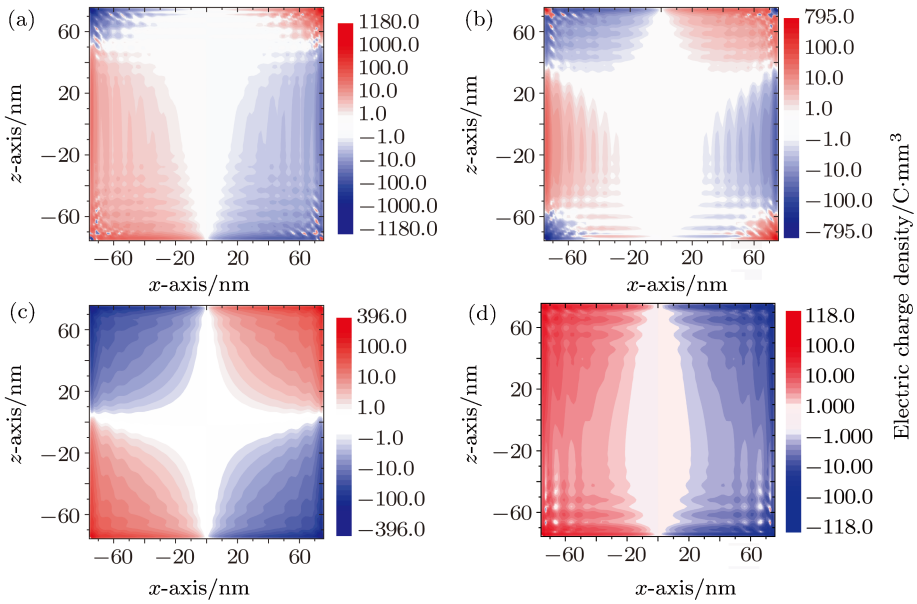

Fig. 4. (Colour online) Electric charge density distributions (in units of C/mm^3, assuming the incident light has $E_0 = 1$ V/m) at the right surface of the nanocube specified in Fig. 3(d), which is within the body of the nanocube. The distance between the plane and the right surface of the nanocube is 2 nm. Panels (a) and (b) both correspond to the wavelength of 495 nm. The picture in panel (b) is recorded a quarter of the time period after that than in (a). Panels (c) and (d) correspond to the wavelengths of 620 nm and 815 nm, respectively.

In both cases, the charges oscillate with time and here we only show their charge distribution at a certain time. We also calculate the charge distribution at the wavelength of 495 nm, which is shown in Fig. 4(a). This mode contains the components of both the dipole mode and the quadrupole mode, and seems to be the mixture of these modes. It might also be a higher order mode. The charges concentrate in the bottom two corners at the time. However, after a quarter the period of time, the charges concentrate in the upper two corners (see Fig. 4(b)). Thus, at the wavelength of 495 nm, there is a $\pi/2$ phase retardation between the charges distributed in the upper corner and the bottom corner. In addition, we note the charge density quantitatively. The maximum charge density is about 1179 C/mm^3 for the 495 nm mode, 395.6 C/mm^3 for the 620 nm mode and 117.9 C/mm^3 for the 815 nm mode when the incident light has an amplitude of $E_0 = 1$ V/m. It is well known that the oscillating charge produces the electric field, and the local field intensity depends dominantly on the extent to which the charges concentrate and how many charges concentrate. The mode excited by the 495 nm incident light can more effectively densify the oscillating charges and this is the reason for the large field enhancement factor.

Until now, we have found that the large electric field enhancement at the wavelength of 495 nm is due to the fact that more charges concentrate in a smaller volume around the corner of the nanocube. At the same time, the field enhancement effect at this wavelength is highly localized in the region very close to the corner, which further enhances the local field intensity. To fully reveal the secret of the LFE-LE peak, we need to further explore the reason why the nanocube has a low extinction cross section at this wavelength.

As the extinction cross section is contributed from two components, which are absorption and scattering cross sections, we will examine both in the following. First, we look at the absorption distribution at the three peaks. Because of the skin effect, the light can hardly reach the interior region of the nanocube. Thus, the absorption mainly takes place in the surface of the nanocube to the extent of the skin depth. Figures 5(a)–5(c) show the absorbed energies of light in a unit volume in the inner surface of the nanocube as specified in Fig. 5(d) at the wavelengths of 495 nm, 620 nm and 815 nm, respectively. Several distinct features can be revealed.

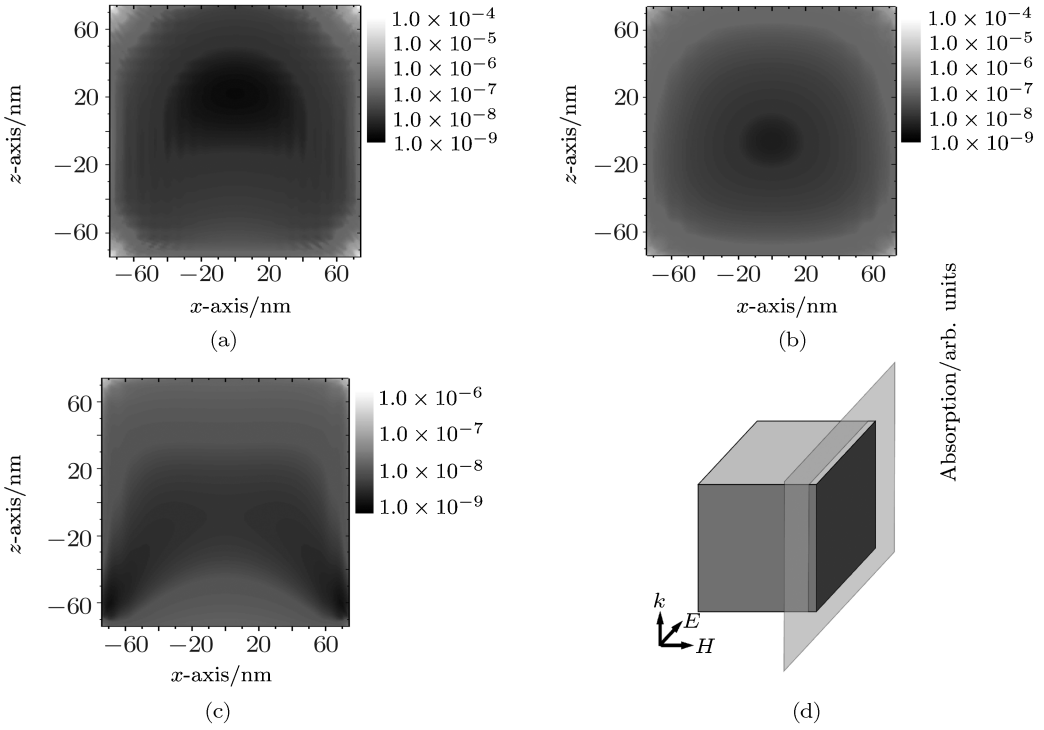

Fig. 5. Absorption distributions in the right surface of the nanocube specified in panel (d) at different incident wavelengths: (a) 495 nm, (b) 620 nm, and (c) 815 nm.

First, we find from Fig. 5(c) that absorption at the 815 nm incident light is quite low. The major reason for this is because the absorptivity of Ag itself is low at this infrared wavelength. Second, comparing the results of Figs. 5(a) and 5(b), we find that at the wavelength of 495 nm the absorption is more concentrated in the corners, which in principle should lead to smaller absorption by the particle. However, since metal is more absorptive in the short wavelength (495 nm) than in the long wavelength (620 nm), the total energy absorbed at 495 nm is still roughly equal to that in the case of the quadrupole mode at 620 nm. In fact, this point also shows up in the calculated optical spectra, as displayed in Fig. 2(e). When one sums up these two aspects, the absorption cross section of the 150 nm Ag nanocube embedded in water under the incident light of 495 nm is at a fairly low level and this surely is one key to the low extinction property of the LFE-LE peak.

Then, we come to another component, the scattering cross section. Although the absorption cross section is at a low level, the low extinction in this strange mode still must be related to the low scattering cross section. On one hand, in principle, the scattering cross section is related to the dipole moment or the quadrupole moment. From the above analysis, we know that the mode at the wavelength of 495 nm is a hybrid resonant mode, which contains both a quadrupole component and a dipole component. This mode brings high electric charge density. However, because the charges appear only in a very limited volume, the total dipole moment and quadrupole moment of this mode are rather small, which may be the main reason for the low extinction cross section. In addition, the contributions from these two modes to scattering of light can be opposite and cancel out each other, which further leads to a small scattering cross section.

On the other hand, we can understand this low scattering cross section from the energy flux distribution. Figures 6(a)–6(c) show the Poynting vectors (in units of the Poynting vector of the incident light) in the surface of the nanocube as specified in Fig. 5(d) at the wavelengths of 495 nm, 620 nm, and 815 nm, respectively. At 495 nm, most of the energy flux of light just passes around the body of the nanocube, except that near the corner the energy flux proceeds in a swirly path circulating around the corner. In the region away from the corner, the light almost propagates along its incident direction straightly and is hardly disturbed. In comparison, for the quadrupole resonant mode (620 nm), the propagating direction of the incident light is changed totally in the upper surface of the nanocube (see Fig. 6(b)) and, for the dipole resonant mode (815 nm), the incident light is affected obviously even at 100 nm away from the nanocube. We know that the total energy flux can be interpreted as the energy sum of the incident light and the scattered light. The more the energy flux is deflected from its initial value, the more the scattered energy is. So, at the wavelength of 495 nm, the total energy flux is influenced very little in the non-near-field region of the nanocube and the scattered energy is small compared with those of the longer wavelength quadrupole and dipole resonant modes. This result also justifies the low scattering cross section at the peak wavelength of 495 nm.

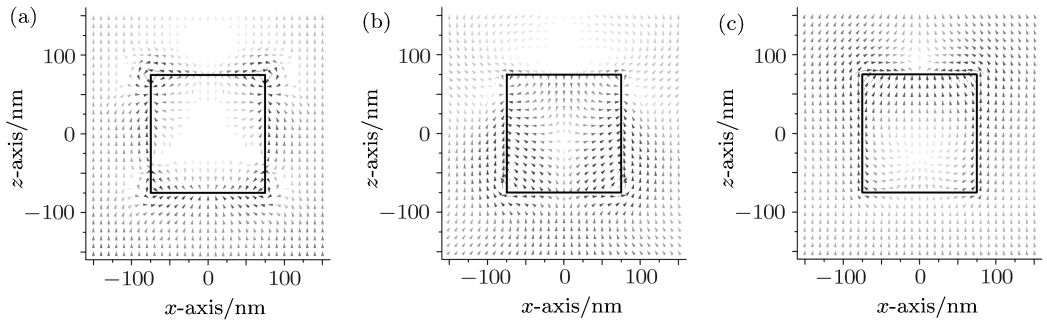

Fig. 6. Energy fluxes (Poynting vectors) in the front surface of the nanocube specified in Fig. 5(d) in units of the incident energy flux at different wavelengths: (a) 495 nm; (b) 620 nm; (c) 815 nm.

4. Conclusions

We have theoretically found in either Ag or Au cubic nanoparticles a novel LFE-LE resonant mode with the peculiar features of a simultaneous large field enhancement factor and low extinction cross section. In order to uncover the physical mechanism, we have analysed this mode from the distribution patterns of local field intensity, energy flux, absorption and charge density. The results show that in the mode the charges are highly densified in a very limited volume around the corner of the nanocube, leading to a very large local enhancement factor of the electric field. On the other hand, the energy flux is only strongly perturbed around the corners in a swirly circulation manner and very weakly influenced away from the corner, which indicates that the scattering effect is small in this mode, leading to a small scattering cross section. In addition, the absorption occurs only in this small volume around the corner, so the absorption cross section is at a low level. All these features contribute to the simultaneous low extinction and the large field enhancement effect at the wavelength of the LFE-LE mode. It is expected that such a strange mode can also be found in metal nanoparticles other than simple nanocubes. Metal nanoparticles with such peculiar properties can be useful for building high-FOM nonlinear optical compound materials with low linear absorption and large nonlinearity.

Appendix: The convergence of DDA method

The convergence of our simulation is checked by comparing the results of the calculation with different inter-dipole spacings, i.e., the grid sizes. Figures A1(a)–A1(c) show the electric field distributions near the cube corner in the surface which is 2 nm away from the cube face (the same as those in Fig. 3) using different inter-dipole spacings of 5 nm, 1.5 nm, 0.75 nm, respectively. Since the nanocube is centred at the origin point, each face is 75 nm in distance from the origin point. We can find that the results obtained by using inter-dipole spacings of 1.5 nm and 0.75 nm are in good agreement with each other, but not with the result obtained by using 5 nm. So we can infer that, for 150 nm Ag nanocubes, the inter-dipole spacing of 5 nm has not yet reached an acceptable accuracy, while that of 1.5 nm can achieve a fine convergence. The error comes from the adjacent effect. The electric field is not reliable at the point too close to a dipole. For the positions a bit farther from the corner, the accuracy should be better.

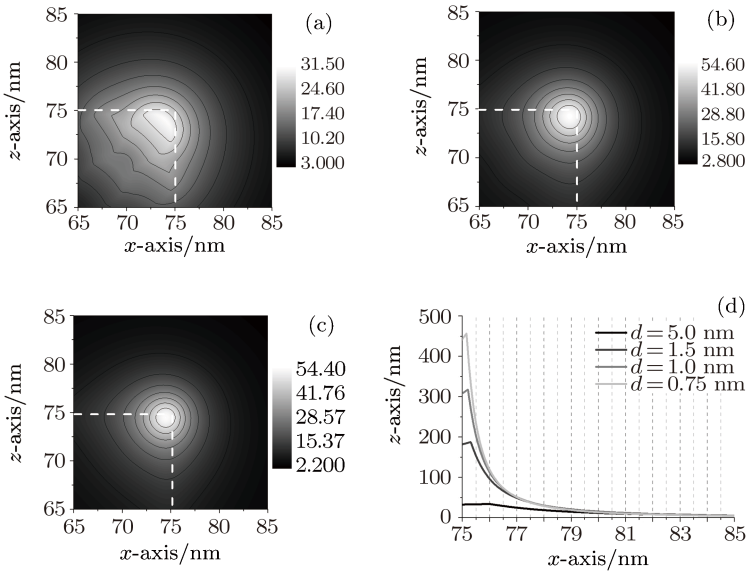

Fig. A1. Electric fields around the corner at the excitation wavelength of 495 nm. Panels (a)–(c) show the electric field distributions in the surface, which are the same as those in Fig. 3 calculated by using inter-dipole spacings of 5.0 nm, 1.5 nm and 0.75 nm, respectively. The white dash lines denote the projection outline of the nanocube. Panel (d) exhibits the electric field along the cube edge which is parallel to x-axis. All the electric fields are in units of E_0, and the coordinate is descripted in Fig. 1.

Then we look in detail at the field distributions at different distances from the nanocube. Figure A1 (d)

shows the electric fields on the edge that is parallel to the x-axis, calculated using different inter-dipole spacings (5 nm, 1.5 nm, 1.0 nm and 0.75 nm, separately). In the region within a distance less than 1 nm from the cube corner, the value is not correct. In the region more than 2 nm from the corner, the results obtained by using spacings of 1.5 nm, 1.0 nm and 0.75 nm are in good agreement with each other. The above analysis indicates that an inter-dipole spacing of 1.5 nm is sufficiently fine to obtain the correct electric field distribution in the surface which is 2 nm in distance from the cube.

References

[1] Chen J Y, Wang D L, Xi J F, Au L, Siekkinen A, Warsen A, Li Z Y, Zhang H, Xia Y N and Li X D 2007 *Nano Letters* **7** 1318

[2] Khlebtsov B, Zharov V, Melnikov A, Tuchin V and Khlebtsov N 2006 *Nanotechnology* **17** 5167

[3] Nam J, Won N, Jin H, Chung H and Kim S 2009 *J. Am. Chem. Soc.* **131** 13639

[4] Patra C R, Bhattacharya R, Mukhopadhyay D and Mukherjee P 2010 *Adv. Drug Deliver. Rev.* **62** 346

[5] Li X, Qian J, Jiang L and He S L 2009 *Appl. Phys. Lett.* **94** 063111

[6] Haes A J, Zou S L, Schatz G C and van Duyne R P 2004 *J. Phys. Chem.* B **108** 109

[7] McLellan J M, Li Z Y, Siekkinen A R and Xia Y N 2007 *Nano Letters* **7** 1013

[8] Doering W E and Nie S M 2002 *J. Phys. Chem.* B **106** 311

[9] Li Z Y and Xia Y N 2010 *Nano Letters* **10** 243

[10] McMahon J M, Henry A I, Wustholz K L, Natan M J, Freeman R G, van Duyne R P and Schatz G C 2009 *Anal. Bioanal. Chem.* **394** 1819

[11] Xing Z W, Wang J R, Ke H T, Zhao B, Yue X L, Dai Z F and Liu J B 2010 *Nanotechnology* **21** 145607

[12] Pustovit V N and Shahbazyan T V 2009 *Phys. Rev. Lett.* **102** 077401

[13] Bharadwaj P and Novotny L 2007 *Opt. Express* **15** 14266

[14] Nishi H, Asahi T and Kobatake S 2009 *J. Phys. Chem.* C **113** 17359

[15] Prodan E, Radloff C, Halas N J and Nordlander P 2003 *Science* **302** 419

[16] Schwartzberg A M, Grant C D, Wolcott A, Talley C E, Huser T R, Bogomolni R and Zhang J Z 2004 *J. Phys. Chem.* B **108** 19191

[17] Halas L, Orinak A, Sharif A, Adamova M and Ladomersky J 2005 *Cent. Eur. J. Chem.* **3** 570

[18] Siu W H and Yu K W 1996 *Phys. Rev.* B **53** 9277

[19] Yuen K P, Law M F, Yu K W and Sheng P 1997 *Phys. Rev.* E **56** R1322

[20] Wang W T, Chen Z H, Yang G, Guan D Y, Yang G Z, Zhou Y L and Lu H B 2003 *Appl. Phys. Lett.* **83** 1983

[21] Yu D B and Yam V W W 2004 *J. Am. Chem. Soc.* **126** 13200

[22] Sun Y G and Xia Y N 2002 *Science* **298** 2176

[23] Sherry L J, Chang S H, Schatz G C, Van Duyne R P, Wiley B J and Xia Y N 2005 *Nano Letters* **5** 2034

[24] Mahmoud M A, Poncheri A J, Phillips R L and El-Sayed M A 2010 *J. Am. Chem. Soc.* **132** 2633

[25] Sosa I O, Noguez C and Barrera R G 2003 *J. Phys. Chem.* B **107** 6269

[26] Galush W J, Shelby S A, Mulvihill M J, Tao A, Yang P D and Groves J T 2009 *Nano Letters* **9** 2077

[27] Zhou F, Li Z Y, Liu Y and Xia Y N 2008 *J. Phys. Chem.* C **112** 20233

[28] Draine B T and Flatau P J 1994 *J. Opt. Soc. Am.* A **11** 1491